nature genetics

p53 deletion impairs clearance of chromosomal-instable stem cells in aging telomere-dysfunctional mice

Yvonne Begus-Nahrmann[1], André Lechel[1], Anna C Obenauf[2], Kodandaramireddy Nalapareddy[1], Elvira Peit[1], Eva Hoffmann[2], Falk Schlaudraff[3], Birgit Liss[3], Peter Schirmacher[4], Hans Kestler[5], Esther Danenberg[6], Nick Barker[6], Hans Clevers[6], Michael R Speicher[2] & K Lenhard Rudolph[1]

Telomere dysfunction limits the proliferative capacity of human cells and induces organismal aging by activation of p53 and p21 (refs. 1–6). Although deletion of p21 elongates the lifespan of telomere-dysfunctional mice[2], a direct analysis of p53 in telomere-related aging has been hampered by early tumor formation in p53 knockout mice[6]. Here we analyzed the functional consequences of conditional p53 deletion[7]. Intestinal deletion of p53 shortened the lifespan of telomere-dysfunctional mice without inducing tumor formation. In contrast to p21 deletion, the deletion of p53 impaired the depletion of chromosomal-instable intestinal stem cells in aging telomere-dysfunctional mice. These instable stem cells contributed to epithelial regeneration leading to an accumulation of chromosomal instability, increased apoptosis, altered epithelial cell differentiation and premature intestinal failure. Together, these results provide the first experimental evidence for an organ system in which p53-dependent mechanisms prevent tissue destruction in response to telomere dysfunction by depleting genetically instable stem cells.

The functional role of p53 in aging is currently under debate. Knock-in mice expressing a hyperactive mutant form of p53 have shown premature aging and reduced lifespan[8]. In contrast, transgenic mice overexpressing an extra copy of naturally regulated, wild-type p53 (encoded by *Trp53*) did not show an alteration in lifespan[9]. Triple transgenic mice overexpressing an extra copy of wild-type p53 along with an

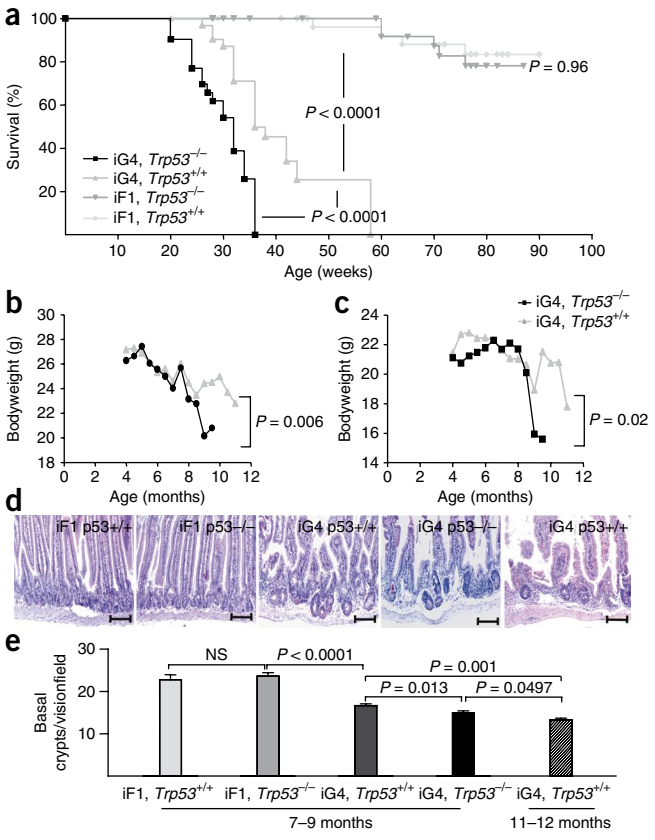

Figure 1 p53 deletion impairs organ maintenance and shortens survival of telomere-dysfunctional mice. (**a**) Kaplan-Meyer curves depicting survival of mice in the indicated cohorts. Survival of iG4 mice ($n = 63$) was lower than that of iF1 mice ($n = 63$, $P < 0.0001$). Note that iG4, *Trp53*$^{-/-}$ mice ($n = 31$) had a significantly shortened lifespan compared to iG4, *Trp53*$^{+/+}$ mice ($n = 32$, $P < 0.0001$). iF1, *Trp53*$^{-/-}$mice ($n = 31$) and iF1, *Trp53*$^{+/+}$ mice ($n = 32$) showed similar survival ($P = 0.345$) during the observation period of 18 months. (**b**,**c**) Weight curves of aging male (**b**) and female (**c**) mice of the iG4, *Trp53*$^{+/+}$ cohort ($n = 17$ and 15, respectively) and the iG4, *Trp53*$^{-/-}$ cohort ($n = 15$ and 16, respectively). Body weights were significantly lower in 8- to 9-month-old iG4, *Trp53*$^{-/-}$ mice compared to iG4, *Trp53*$^{+/+}$ mice ($P = 0.006$ males, $P = 0.0154$ females, aged 9 months). (**d**) Representative hematoxylin and eosin (H&E) staining from small intestine. Scale bar, 200 µm. (**e**) The number of basal crypts per vision field. Crypt numbers were lower in iG4 mice ($n = 16$) compared to iF1 mice ($n = 10$, $P < 0.0001$). Seven- to nine-month-old iG4, *Trp53*$^{-/-}$ mice ($n = 8$) showed a lower number of crypts compared to age-matched iG4, *Trp53*$^{+/+}$ mice ($n = 8$, $P = 0.013$). As a control, we examined the crypt number of 11- to 12-month-old iG4, *Trp53*$^{+/+}$ ($n = 5$–8 mice).

[1]Institute of Molecular Medicine and Max-Planck-Research Department on Stem Cell Aging, University of Ulm, Ulm, Germany. [2]Institute of Human Genetics, Medical University of Graz, Graz, Austria. [3]Institute of General Physiology, University of Ulm, Ulm, Germany. [4]Institute of Pathology, University Hospital, Heidelberg, Germany. [5]Institute for Neuroinformatics, University of Ulm, Ulm, Germany, [6]Hubrecht Institute, Utrecht, The Netherlands. Correspondence should be addressed to K.L.R. (lenhard.rudolph@uni-ulm.de).

Received 24 April; accepted 29 June; published online 30 August 2009; doi:10.1038/ng.426

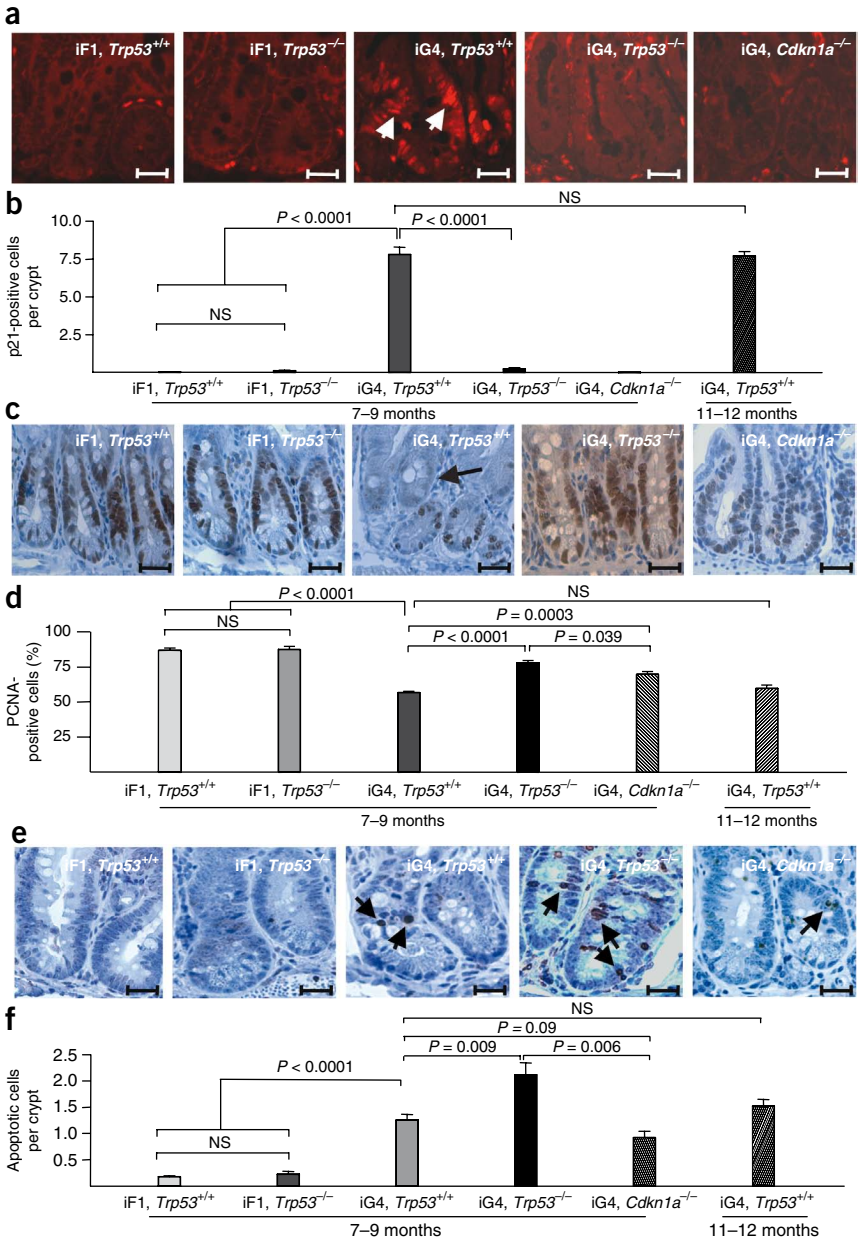

Figure 2 p53 deletion rescues cell cycle arrest but increases apoptosis in telomere-dysfunctional intestine. (**a**,**b**) Expression of p21 in basal intestinal crypts. (**a**) Representative immunohistochemistry (IHC) against p21. White arrows point to p21-positive cells; scale bar, 50 µm. (**b**) The percentage of p21-positive cells per crypt in the small intestine of mice ($n = 5$ mice per group). iG4 mice displayed an increase in p21-positive cells per crypt, which was rescued in iG4, $Trp53^{-/-}$ mice ($P < 0.0001$). (**c**,**d**) Cell proliferation in basal intestinal crypts. (**c**) Representative IHC against PCNA. Black arrow points to a PCNA-negative crypt; scale bar, 50 µm. (**d**) The percentage of PCNA-positive cells in basal crypts of mice ($n = 5$ mice per group). Seven- to nine-month-old iG4, $Trp53^{+/+}$ mice showed a reduction in PCNA-positive crypt cells, which were partially rescued in iG4 $Trp53^{-/-}$ mice ($P < 0.0001$) and iG4, $Cdkn1a^{-/-}$ mice ($P = 0.0003$). (**e**,**f**) Apoptosis in basal intestinal crypts. (**e**) Representative TUNEL staining. Black arrows point to TUNEL-positive cells; scale bar, 50 µm. (**f**) The number of apoptotic cells per crypt in the small intestine of mice ($n = 5$ mice per group). Seven- to nine-month-old iG4, $Trp53^{+/+}$ mice displayed an increase in TUNEL-positive cells, which was further increased in iG4, $Trp53^{-/-}$ mice ($P = 0.009$) but not in iG4, $Cdkn1a^{-/-}$ mice ($P = 0.100$).

extra copy of the cell cycle inhibitors $p19^{ARF}$ and p16 showed an increased lifespan[10] that was even more pronounced when the catalytic subunit of telomerase (TERT) was introduced as a fourth transgene[11]. It appears that p53 by itself can have different effects on aging depending on gene expression, protein activity and the molecular context.

One important molecular component of human aging is the accumulation of telomere dysfunction and DNA damage[12–14]. Telomeres shorten in most human tissues during aging, and there is growing evidence for an accumulation of telomere dysfunction and DNA damage in human aging and age-associated diseases[12,14]. Studies in late-generation telomerase knockout mice (G3–G6 $Terc^{-/-}$) have shown that telomere dysfunction can limit stem cell function, organ maintenance and lifespan[2–5]. In cell culture, telomere dysfunction induces p53-dependent DNA damage checkpoints, including p21-dependent senescence[1,15]. Deletion of p21 (encoded by *Cdkn1a*) abrogates cell cycle arrest, improves organ maintenance and elongates the lifespan of telomere-dysfunctional mice[2].

Studies on human fibroblasts have shown that p53-independent checkpoints limit the survival of telomere-dysfunctional cells that have bypassed senescence. This checkpoint is named 'crisis' and is characterized by an accumulation of telomere dysfunction, chromosomal instability and cell death[1]. *In vivo*, crisis involves the following two checkpoint stages, which limit the survival of germ cells and tumor cells in response to telomere dysfunction and genomic instability: a p53-dependent checkpoint at early stages of genomic instability and a p53-independent checkpoint in response to high levels of genomic instability[6]. The role of p53-dependent checkpoints in the aging of somatic tissues in the context of telomere dysfunction remains to be defined. Of note, overexpression of an extra copy of naturally regulated, wild-type p53 did not affect the lifespan of telomere-dysfunctional mice[16].

Here we crossed late-generation telomerase knockout mice (G3 $Terc^{-/-}$) carrying two floxed alleles of *Trp53* ($Trp53^{loxP/loxP}$)[7] with compound mutant $Terc^{+/-}$; $Trp53^{loxP/loxP}$ mice carrying an inducible Cre-recombinase transgene ($Cre\text{-}ER^{T2}$) under control of the villin promoter[17], which is specifically active in the intestinal epithelium (**Supplementary Figs. 1** and **2a**,**b**). These crosses generated the following cohorts ($Trp53^{-/-}$, homozygous deletion of exons 2–10 of *Trp53* in the intestinal epithelium; iF1, intercross $Terc^{+/-}$ offspring; iG4, intercross $Terc^{-/-}$ offspring): (i) iF1, $Trp53^{+/+}$ ($n = 31$), (ii) iF1, $Trp53^{-/-}$ ($n = 32$), (iii) iG4, $Trp53^{+/+}$ ($n = 32$), (iv) iG4, $Trp53^{-/-}$ ($n = 31$).

Consistent with previous studies[2,5], telomere-dysfunctional iG4 mice had a significantly shortened lifespan compared to iF1 littermates with functional telomeres (**Fig. 1a**, $P < 0.0001$). Intestinal

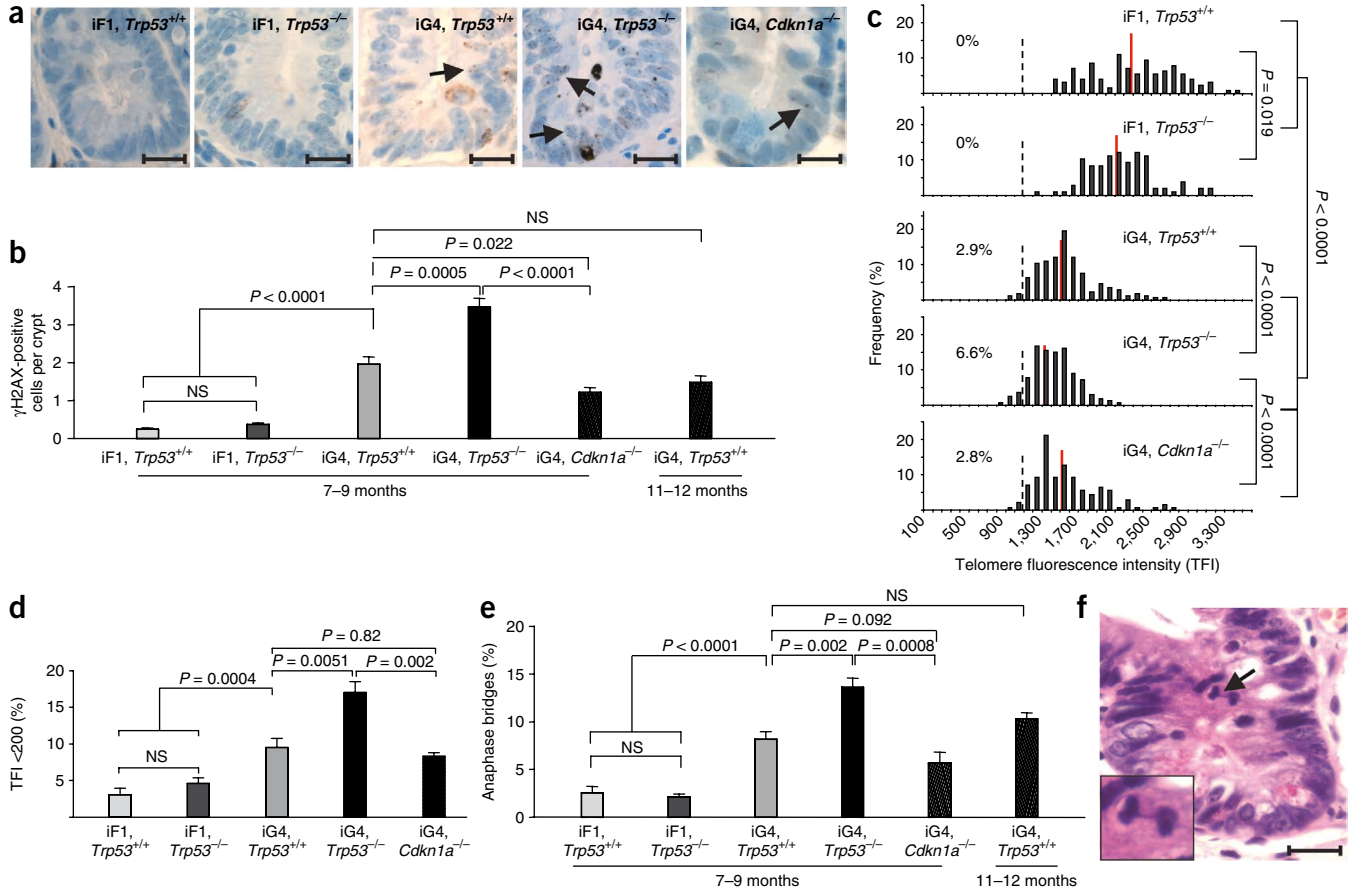

Figure 3 p53 deletion increases the accumulation of telomere dysfunction and DNA damage in intestinal epithelium of iG4 mice. (**a**,**b**) DNA breaks in basal intestinal crypts. (**a**) Representative IHC showing nuclear γ-H2AX foci. Arrows point to γH2AX-positive cells; scale bar, 50 μm. (**b**) The number of γH2AX-positive cells per crypt in the small intestine of mice of the indicated genotype and age (n = 5–8 mice per group). Note that p53 deletion increased the number of γH2AX-positive cells in iG4 mice (P = 0.0005), which was not observed in response to p21 deletion. (**c**,**d**) Telomere length in basal intestinal crypts of 7- to 9-month-old mice. (**c**) The distribution of the mean telomere fluorescence intensity (TFI) of individual crypts of mice of the indicated genotype (n = 5 mice per group, n = 30 crypts per mouse). The red line shows the mean TFI of individual crypts, the number left of the dotted line shows the percentage of crypts with critically short telomeres. (**d**) The prevalence of individual telomere spots with a very low fluorescence intensity (<200 arbitrary units). (**e**) The percentage of cells in anaphase showing chromatin bridges in intestinal basal crypts of mice (n = 5–8 mice per group). Within the iG4 cohort, p53 deletion increased the percentage of anaphase bridges (P = 0.002), whereas p21 deletion had no significant effect (P = 0.093). (**f**) Representative H&E staining showing an anaphase bridge (black arrow) in the small intestine. Scale bar, 50 μm (inset, 100 μm).

deletion of p53 had no effect on lifespan of iF1 mice, but the deletion significantly shortened the lifespan of iG4, *Trp53*$^{-/-}$ mice compared to iG4, *Trp53*$^{+/+}$ mice (**Fig. 1a**, $P < 0.0001$). The shortened lifespan of iG4, *Trp53*$^{-/-}$ mice was not associated with tumor formation, on either a macroscopic or a histological level (data not shown). Seven- to nine-month-old iG4, *Trp53*$^{-/-}$ mice showed an acceleration of intestinal crypt atrophy and weight loss compared to age-matched iG4, *Trp53*$^{+/+}$ mice (**Fig. 1b–e** and **Supplementary Fig. 2c**,**d**). Premature crypt atrophy correlated with increased inflammation in the intestinal epithelium of 7- to 9-month-old iG4, *Trp53*$^{-/-}$ mice (**Supplementary Table 1**), possibly due to a decrease in intestinal barrier function.

The observed effects of intestinal p53 deletion here were very different from previous studies on p21 deletion, which resulted in improved maintenance of the intestinal epithelium and an elongated lifespan of telomere-dysfunctional mice[2]. Here p53 deletion prevented the upregulation of p21 in intestinal basal crypts of aging iG4 mice (**Fig. 2a**,**b**), which correlated with a significant rescue in cell proliferation in the basal intestinal crypts of the mice (**Fig. 2c**,**d** and **Supplementary Fig. 3a–c**, $P < 0.0001$). Expression analysis of phosphorylated histone H3 revealed a very low increase in the incidence of G2/M arrested cells (<2%) in the intestinal epithelium of iG4, *Trp53*$^{+/+}$ mice (**Supplementary Fig. 3d**), indicating that telomere dysfunction in intestinal epithelium of iG4 mice induced primarily a p53- and p21-dependent G1 cell cycle arrest. In contrast to p21 deletion[2], the deletion of p53 did not improve maintenance of the intestinal epithelium of iG4 mice (**Fig. 1b–d** and **Supplementary Fig. 2c**,**d**), indicating that p53 deletion had adverse effects counteracting the impairment in p21 induction and the rescue of cell proliferation.

Our previous studies have shown that p21 deletion rescued cell proliferation, maintenance of the intestinal epithelium and lifespan of iG4 mice[2]. However, this rescue was limited by an increase in apoptosis occurring at the end of the extended lifespan in the intestine of 20-month-old iG4, *Cdkn1a*$^{-/-}$ mice[2]. This delayed increase in apoptosis stood in agreement with the classical experiments in human fibroblasts that showed that abrogation of p53 or p21 leads to a bypass of the senescence checkpoint. However, the extended lifespan of these cells was limited by mitotic catastrophe–induced cell death (crisis) several population doublings after bypass of the senescence checkpoint[1,15]. In contrast to the delayed apoptosis response in 20-month-old iG4, *Cdkn1a*$^{-/-}$ mice, our study revealed that the intestinal deletion of p53 induces an early increase in apoptosis in basal crypts of 7- to 9-month-old iG4, *Trp53*$^{-/-}$ mice compared to age-matched iG4, *Trp53*$^{+/+}$ and iG4, *Cdkn1a*$^{-/-}$ mice (**Fig. 2e**,**f**).

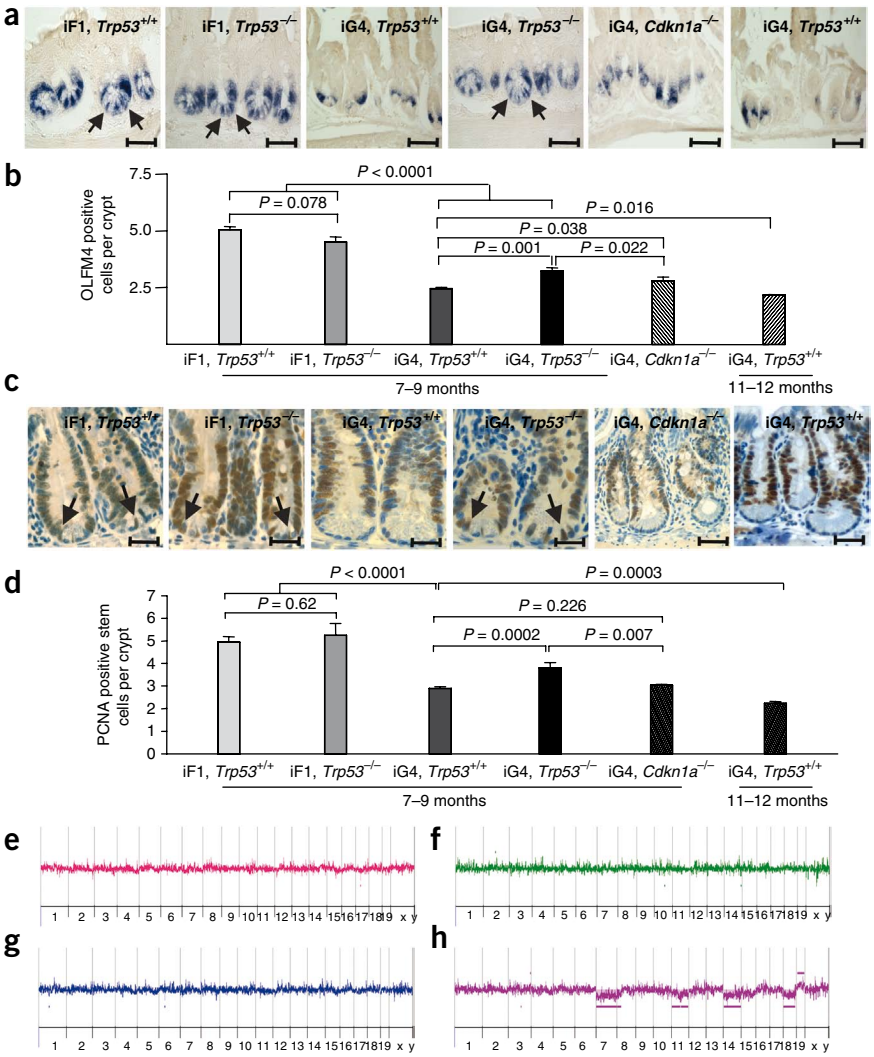

Figure 4 p53 deletion impairs the depletion of stem cells and increases chromosomal instability in basal crypts of telomere-dysfunctional mice. (**a**–**d**) Intestinal stem cells in basal crypts. (**a**) Representative *in situ* staining of OLFM4-positive stem cells in basal intestinal crypts. Black arrows point to OLFM4-positive stem cells; scale bar, 50 μm. (**b**) The number of OLFM4-positive intestinal stem cells in basal crypts of the small intestine of mice of the indicated age and genotype (n = 4–6 mice per group). Within the iG4 cohorts, p53 deletion increased the stem cell number (P = 0.001). p21 deletion also led to a partial rescue in OLFM4-positive cells, but the number remained lower than that in iG4, $Trp53^{-/-}$ mice (P = 0.022). (**c**) Representative IHC showing PCNA-positive stem cells at the bottom of basal intestinal crypts. Black arrows point to PCNA-positive stem cells; scale bar, 50 μm. (**d**) The number of PCNA-positive intestinal stem cells in basal crypts of the small intestine of mice of the indicated age and genotype (n = 5–8 mice per group). Within the iG4 cohorts, p53 deletion increased the stem cell number (P = 0.0002), whereas p21 deletion had no effect (P = 0.226). (**e**–**h**) Representative genome-wide array-CGH profiles obtained from single colonic crypts from (e) iF1, $Trp53^{+/+}$, (f) iF1, $Trp53^{-/-}$, (g) iG4, $Trp53^{+/+}$, (h) iG4, $Trp53^{-/-}$ mice. Whereas the first three profiles are balanced, the last ratio profile (**h**) shows several imbalances (purple bars).

To reveal the underlying mechanism of the early increase in apoptosis in the intestine of iG4, $Trp53^{-/-}$ mice, we determined the accumulation of DNA damage and telomere dysfunction in 7- to 9-month-old mice. γH2AX staining revealed significantly increased rates of DNA damage in intestinal epithelial cells of iG4, $Trp53^{-/-}$ mice compared to iG4, $Trp53^{+/+}$ mice (P = 0.0005) and iG4, $Cdkn1a^{-/-}$ mice (P < 0.0001, **Fig. 3a**,**b**). Moreover, a significant increase of cells with critically short telomeres occurred in the intestinal epithelium of iG4, $Trp53^{-/-}$ mice compared to iG4, $Trp53^{+/+}$ mice (P = 0.0051) and iG4, $Cdkn1a^{-/-}$ mice (P = 0.002, **Fig. 3c**,**d**). In addition, the number of anaphase bridges—which are hallmarks of telomere dysfunction and chromosomal fusion[18]—was significantly increased in intestinal basal crypts of iG4, $Trp53^{-/-}$ mice compared to iG4, $Trp53^{+/+}$ mice (P = 0.002) and iG4, $Cdkn1a^{-/-}$ mice (P = 0.0008, **Fig. 3e**,**f**). Control experiments excluded effects of Cre expression on apoptosis, DNA damage and anaphase bridge formation (**Supplementary Fig. 4a–h**). Together, these data indicate that p53 has a p21-independent function preventing survival of epithelial cells that carry dysfunctional telomeres or DNA damage.

To analyze at which level in the cellular hierarchy p53 prevented survival of damaged cells, we determined the number of intestinal stem cells by PCNA staining[19] and OLFM4 *in situ* hybridization in 7- to 9-month-old mice[20]. Significantly fewer intestinal stem cells were seen in iG4, $Trp53^{+/+}$ mice compared to iF1 mice (**Fig. 4a–d**, P < 0.0001). Deletion of p53 had no significant effect on stem cell numbers in iF1 mice but significantly rescued the decline in stem cell number in basal crypts of iG4 mice (**Fig. 4a–d**, P = 0.001 for OLFM4-positive cells, P = 0.0002 for PCNA-positive cells). Of note, the number of intestinal stem cells was also greater in iG4, $Trp53^{-/-}$ mice compared to iG4, $Cdkn1a^{-/-}$ mice (**Fig. 4b**,**d**, P = 0.022 for OLFM4-positive cells, P = 0.007 for PCNA-positive cells), suggesting that prolonged survival of damaged stem cells may occur in the intestine of telomere-dysfunctional mice in response to p53 deletion but not in response to p21 deletion.

To test this hypothesis, we performed array-comparative genomic hybridization (array-CGH) on micro-dissected basal crypts of 7- to 9-month-old mice. Each intestinal crypt represents a self-renewing unit generated from a few intestinal stem cells. We reasoned that genomic instability at the single crypt level (20–30 cells) should only be detectable when genetically instable stem cells regenerated the crypt but not when random instability occurred at the level of progenitor cells. We detected a high incidence of chromosomal gains and losses in crypts of 7- to 9-month-old iG4, $Trp53^{-/-}$ mice, but such gains and losses rarely occurred in the other cohorts (**Figs. 4e–h** and **5a**, and **Table 1**). Control experiments excluded an effect of Cre expression on the induction of chromosomal imbalances (**Supplementary Fig. 5**). Conventional fluorescence *in situ* hybridization (FISH) confirmed an increased incidence of chromosomal aberrations in intestinal crypts of iG4, $Trp53^{-/-}$ mice but stable chromosome copy numbers in iG4, $Cdkn1a^{-/-}$ mice, including the oldest survivors in this cohort at 20 months of age (**Fig. 5b** and **Supplementary Fig. 6a**). Together, these data indicate that chromosomal instability occurred in intestinal stem cells of aging iG4, $Trp53^{-/-}$ mice but not in the other cohorts,

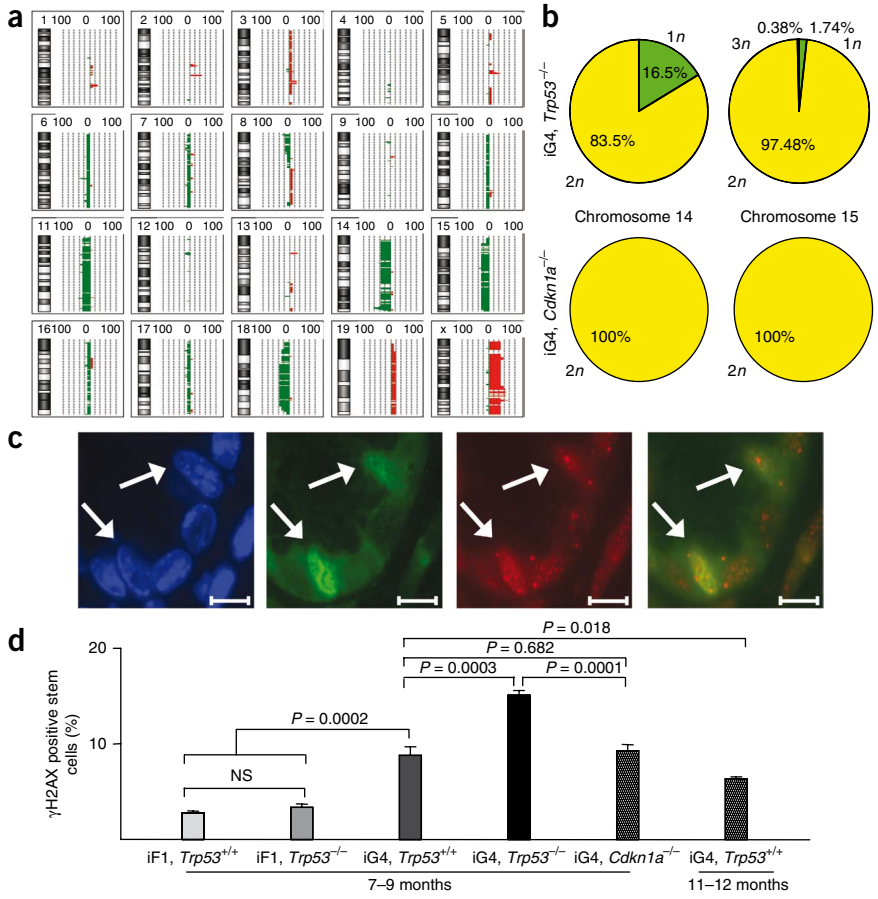

Figure 5 p53 deletion, but not p21 deletion, increases survival of chromosomal-instable stem cells in basal intestinal crypts of telomere-dysfunctional mice. (**a**) Summary of chromosomal gains and losses in basal crypts of 7- to 9-month-old iG4, *Trp53*$^{-/-}$ mice. The bars on the right side of each chromosome indicate how often (in what percentage) a gain or loss was found. Losses are displayed in green in the left half of the bars, and gains are shown in red in the right half. Some changes, such as loss of chromosomes 11 and 14 or the loss of the proximal region of chromosome 8, were recurrently observed, whereas other changes occurred only once. (**b**) The percentage of chromosomal gains and losses of chromosome 14 and 15 in basal crypts of iG4, *Trp53*$^{-/-}$ and iG4, p21$^{-/-}$ mice analyzed by FISH. (**c**,**d**) p53 deletion increases DNA damage in intestinal stem cells of 7- to 9-month-old telomere-dysfunctional mice. (**c**) Representative IHC showing γH2AX-positive intestinal stem cells (PCNA-positive in positions 1–4 at the bottom of the crypt) in the small intestine. Scale bar, 10 μm. (**d**) The percentage of γH2AX-positive stem cells in mice. iG4 mice showed an increase in DNA damage foci in intestinal stem cells compared to iF1 mice. Within the iG4 cohort, p53 deletion increased the percentage of intestinal stem cells showing DNA damage foci ($P = 0.0003$), whereas p21 deletion had no significant effect ($P = 0.682$).

including that of iG4, *Cdkn1a*$^{-/-}$ mice. In agreement with this interpretation, γH2AX and PCNA co-staining revealed that p53 deletion increased the rate of DNA damage in intestinal stem cells of aged iG4 mice, whereas p21 deletion had no significant effect (**Fig. 5c**,**d**).

The imbalance in expression of various genes arising from duplications and/or deletions of entire chromosomes could contribute to compromised tissue integrity in aging iG4, *Trp53*$^{-/-}$ mice either by increasing the mice's susceptibility to environmental stress and non-specific cell death (see above data on apoptosis) or through altered epithelial cell differentiation. In agreement with the latter assumption, RNA expression analysis and protein marker analysis here revealed alterations in epithelial cell differentiation in the intestine of iG4, *Trp53*$^{-/-}$ mice compared to iG4, *Trp53*$^{+/+}$ mice (**Supplementary Fig. 6b**,**c** and **Supplementary Table 2**).

Our study provides experimental evidence that deletion of p53 compromises the integrity of the intestinal epithelium of aging telomere-dysfunctional mice. There is growing evidence that a decrease in stem cell function contributes to an impairment in maintenance and function of somatic organs during aging[21,22]. The current findings indicate that p53 is required to deplete intestinal stem cells carrying DNA breaks and chromosomal aberrations. Our findings could provide an explanation for the delayed onset of age-related gene expression changes in hematopoietic stem cells of aging mice with superactive p53 compared to wild-type mice[23]. However, accelerated aging in mouse mutants with superactive p53 (ref. 8) indicates that the function of p53 in depleting damaged stem cells needs to stay within certain levels. An overactivation of this pathway may reduce stem cell numbers prematurely, whereas a loss of p53 function leads to survival of dysfunctional and damaged stem cells.

Our study shows that p53 deletion leads to survival of chromosomal-instable stem cells in telomere-dysfunctional mice. The type of genomic instability in this model mostly involves entire chromosomes and could possibly represent a specific type of genomic instability

Table 1 Genomic imbalance in basal crypts of iG4, Trp53$^{-/-}$ mice

	iG4 *Trp53*$^{-/-}$					
	Duplication			Deletion		
Chr.	Whole chr.	Partial	Total #	Whole chr.	Partial	Total #
1		1	1			
2						
3						
4						
5		2	2			
6				1		1
7				1		1
8		1	1		1	1
9						
10	1		1		1	1
11	1	2	3			
12					1	1
13		1	1			
14				4		4
15				1	2	3
16				1		1
17				1		1
18				1	3	4
19	2		2			

The table displays all chromosomal aberrations detected in basal crypts of 7- to 9-month-old iG4, *Trp53*$^{-/-}$ mice ($n = 9$ crypts).

induced by end-to-end fusions in telomere-dysfunctional tissues. In human cancers, the complexity of chromosomal aberrations is often higher involving gains and losses of chromosomal fragments, inversions, duplications and translocations. An increased complexity in chromosomal aberrations in human cancer in response to telomere dysfunction might be due to an increased formation of dicentric chromosomes that are instable and prone to breakage[24].

Our study shows that the survival of instable stem cells is disadvantageous at the tissue level, and that this survival leads to aberrant differentiation, increased rates of apoptosis and premature organ failure. Recent studies have revealed a decline in p53 checkpoint function in aging mice and a correlation between the onset of this decline in checkpoint function and the lifespan of various mouse strains[25]. Impaired clearance of damaged stem cells may contribute to tissue degeneration and lifespan reduction in response to an age-dependent decline in p53 checkpoint function.

Previous studies have shown a protective role of p53- and p21-dependent cell cycle arrest in acute intestinal injury induced by high-dose irradiation[26]. Our results differ from these previous results and provide to our knowledge the first evidence that p53 has a unique function in maintaining a genetically stable stem cell pool in telomere-dysfunctional intestine. This specific function of p53 is independent of p21-induced cell cycle arrest and may involve other processes controlled by p53, such as apoptosis[6]. These findings support the concept that p53-dependent checkpoints are activated at early stages of telomere dysfunction–induced crisis *in vivo*[6]. According to our results, these p53-dependent responses ensure the depletion of chromosomal-instable stem cells in telomere-dysfunctional intestine. Previous studies on telomere-dysfunctional mice have shown that p53 deletion can also have beneficial effects on organ maintenance by rescuing germ cell apoptosis and fertility as well as epidermal stem cell function[6,27]. These data indicate that the adverse effects of p53 deletion induced by impaired clearance of genetically instable stem cells can show tissue specificity. Our findings appear to be highly relevant in defining molecular targets for future therapies aiming to improve tissue regeneration in the context of telomere dysfunction and aging. Moreover, our findings point to an alternative pathway in intestinal carcinogenesis, indicating that chromosomal-instable stem cells can clonally expand and thus can contribute to epithelial regeneration at pre-tumorous stages.

METHODS

Methods and any associated references are available in the online version of the paper at http://www.nature.com/naturegenetics/.

Note: Supplementary information is available on the Nature Genetics website.

ACKNOWLEDGMENTS

We thank S. Robine (Institute Curie-CNRS, Paris) for providing villin-Cre-ERT2 mice and A. Berns (The Netherlands Cancer Institute, Amsterdam) for providing conditional p53 knockout mice. We thank J. Jonkers ((The Netherlands Cancer Institute, Amsterdam) for providing the BAC clones for chromosome FISH. We thank G. Schütz (German Cancer Research Center, Heidelberg) for providing self-made Cre antibody. We thank C. Günes for critical reading of the manuscript. This project was supported by funding from the Deutsche Forschungsgemeinschaft (KFO 167, RU745/10-1), by the Deutsche Krebshilfe e.V. (consortium grant on tumor stem cells) and by the European Union (GENINCA, Telomarker). K.L.R. and M.R.S. are both supported by the European Union (GENINCA, contract number 202230).

AUTHOR CONTRIBUTIONS

Y.B.-N. conducted experiments and data analysis; A.L. and E.P. conducted the chromosome FISH; A.C.O., M.R.S. and E.H. conducted array-CGH analysis; K.N. and P.S. did the analysis of intestinal atrophy and pathology; F.S. and B.L. conducted the laser microdissection of intestinal crypts; H.K. was responsible for the bioinformatics; E.D., N.B. and H.C. conducted the OLFM4 *in situ*; K.L.R. was responsible for the study design and manuscript preparation.

Published online at http://www.nature.com/naturegenetics/.
Reprints and permissions information is available online at http://npg.nature.com/reprintsandpermissions/.

1. Wright, W.E. & Shay, J.W. The two-stage mechanism controlling cellular senescence and immortalization. *Exp. Gerontol.* **27**, 383–389 (1992).
2. Choudhury, A.R. *et al.* Cdkn1a deletion improves stem cell function and lifespan of mice with dysfunctional telomeres without accelerating cancer formation. *Nat. Genet.* **39**, 99–105 (2007).
3. Rudolph, K.L. *et al.* Longevity, stress response, and cancer in aging telomerase-deficient mice. *Cell* **96**, 701–712 (1999).
4. Schaetzlein, S. *et al.* Exonuclease-1 deletion impairs DNA damage signaling and prolongs lifespan of telomere-dysfunctional mice. *Cell* **130**, 863–877 (2007).
5. Hemann, M.T. *et al.* The shortest telomere, not average telomere length, is critical for cell viability and chromosome stability. *Cell* **107**, 67–77 (2001).
6. Chin, L. *et al.* p53 deficiency rescues the adverse effects of telomere loss and cooperates with telomere dysfunction to accelerate carcinogenesis. *Cell* **97**, 527–538 (1999).
7. Jonkers, J. *et al.* Synergistic tumor suppressor activity of BRCA2 and p53 in a conditional mouse model for breast cancer. *Nat. Genet.* **29**, 418–425 (2001).
8. Tyner, S.D. *et al.* p53 mutant mice that display early ageing-associated phenotypes. *Nature* **415**, 45–53 (2002).
9. Garcíía-Cao, I. *et al.* "Super p53" mice exhibit enhanced DNA damage response, are tumor resistant and age normally. *EMBO J.* **21**, 6225–6235 (2002).
10. Matheu, A. *et al.* Delayed ageing through damage protection by the Arf/p53 pathway. *Nature* **448**, 375–379 (2007).
11. Tomás-Loba, A. *et al.* Telomerase reverse transcriptase delays aging in cancer-resistant mice. *Cell* **135**, 609–622 (2008).
12. Jiang, H. *et al.* Proteins induced by telomere dysfunction and DNA damage represent biomarkers of human aging and disease. *Proc. Natl. Acad. Sci. USA* **105**, 11299–11304 (2008).
13. Lieber, M.R. & Karanjawala, Z.E. Ageing, repetitive genomes and DNA damage. *Nat. Rev. Mol. Cell Biol.* **5**, 69–75 (2004).
14. Nalapareddy, K. *et al.* Determining the influence of telomere dysfunction and DNA damage on stem and progenitor cell aging - what markers can we use? *Exp. Gerontol.* **43**, 998–1004 (2008).
15. Brown, J.P., Wei, W. & Sedivy, J.M. Bypass of senescence after disruption of p21CIP1/WAF1 gene in normal diploid human fibroblasts. *Science* **277**, 831–834 (1997).
16. García-Cao, I. *et al.* Increased p53 activity does not accelerate telomere-driven ageing. *EMBO Rep.* **7**, 546–552 (2006).
17. el Marjou, F. *et al.* Tissue-specific and inducible Cre-mediated recombination in the gut epithelium. *Genesis* **39**, 186–193 (2004).
18. Rudolph, K.L. *et al.* Telomere dysfunction and evolution of intestinal carcinoma in mice and humans. *Nat. Genet.* **28**, 155–159 (2001).
19. Barker, N. *et al.* Identification of stem cells in small intestine and colon by marker gene Lgr5. *Nature* **449**, 1003–1007 (2007).
20. van der Flier, L.G. *et al.* Transcription factor achaete scute-like 2 controls intestinal stem cell fat. *Cell* **136**, 903–912 (2009).
21. Rando, T.A. Stem cells, ageing and the quest for immortality. *Nature* **441**, 1080–1086 (2006).
22. Sharpless, N.E. & DePinho, R.A. How stem cells age and why this makes us grow old. *Nat. Rev. Mol. Cell Biol.* **8**, 703–713 (2007).
23. Chambers, S.M. *et al.* Aging hematopoietic stem cells decline in function and exhibit epigenetic dysregulation. *PLoS Biol.* **5**, e201 (2007).
24. Riboni, R. *et al.* Telomeric fusions in cultured human fibroblasts as a source of genomic instability. *Cancer Genet. Cytogenet.* **95**, 130–136 (1997).
25. Feng, Z. *et al.* Declining p53 function in the aging process: a possible mechanism for the increased tumor incidence in older populations. *Proc. Natl. Acad. Sci. USA* **104**, 16633–16638 (2007).
26. Komarova, E.A. *et al.* Dual effect of p53 on radiation sensitivity in vivo: p53 promotes hematopoietic injury, but protects from gastro-intestinal syndrome in mice. *Oncogene* **23**, 3265–3271 (2004).
27. Flores, I. & Blasco, M.A. A p53-dependent response limits epidermal stem cell functionality and organismal size in mice with short telomeres. *PLoS One* **4**, e4934 (2009).

ONLINE METHODS

Mouse crosses and survival. *Trp53*$^{loxP/loxP}$ were crossed with *Terc*$^{+/-}$ mice to generate *Terc*$^{+/-}$; *Trp53*$^{loxP/loxP}$ mice. These mice were crossed through successive generations to produce G3 *Terc*$^{-/-}$; *Trp53*$^{loxP/loxP}$ mice. Intercrosses between *Terc*$^{+/-}$; *Trp53*$^{loxP/loxP}$; villin-Cre-ERT2^{+} and G3 *Terc*$^{-/-}$; *Trp53*$^{loxP/loxP}$ mice were carried out to obtain the experimental cohorts (**Supplementary Fig. 1**). At 4 weeks of age, all mice were injected with 1 mg of tamoxifen (intraperitoneally, five times in daily intervals). Mice were maintained on C57BL/6J background. The animal experiments were approved by the government of the state of Baden-Württemberg (animal protocol number 35/915.81-3).

Histopathological examination of tissues. For survival analysis, aging cohorts were monitored by weekly inspections. Mice were killed after losing >25% of body weight or when mice were moribund. In addition, a cohort of mice ($n = 7$) was killed at 7–9 months of age to retrieve various organs for histological analysis. Organs were fixed in 4% (vol/vol) buffered formalin overnight or snap frozen in liquid nitrogen. Whole mounts of colon were prepared as previously described[2].

Immunohistochemistry on paraffin sections. 5-µm-thick sections of the prepared organs were deparaffinized and rehydrated. For antigen retrieval, sections were pressure cooked in citrate buffer (pH 6.0). Sections were stained with the following primary antibodies overnight at 4 °C: anti-PCNA (Oncogene), anti-p53 (Zymed), anti-p21 (Santa Cruz), anti-γH2AX (Millipore), anti pH3 (Santa Cruz), anti Ki67 (Monosan), chromogranin A (Abcam) and anti-Cre (kind gift from G. Schütz lab, German Cancer Research Center, Heidelberg). Apoptosis was measured using a TUNEL assay kit (Roche). For PCNA, p53, Cre and γH2AX, a biotinylated secondary antibody and the vectastain ABC elite kit (Vector Laboratories) were used. For p21, a secondary antibody labeled with Cy3 was used. Staining was analyzed in a minimum of 200 crypts per mouse.

Quantitative fluorescence *in situ* hybridization (qFISH) for telomere length. Q-FISH was performed on 5-µm paraffin sections of the organs according to previous protocols[2,4] using a cye3-labeled PNA probe (Panagene). The relative telomere length was measured by the telomere fluorescence intensity by a TFL analysis software program[28].

Chromosome FISH. Sections were treated as described above. Additionally, these sections were incubated with proteinase K (1 mg/ml). The hybridization mix (50 vol/vol formamide; 4× citrate buffered saline (SSC) buffer; 80 µg/ml Cot1 mouse DNA; 400 µg/ml herring sperm; 1× Denhardt solution; 20 nM CHAPS; 5 mM EDTA; 400 ng of Cy3-labeled probe; for chromosome 14 the RP23-338A21 BAC clone and for chromosome 15 the RP23-299O23 BAC clone was used[29]) was added and slides were covered with coverslips. The DNA was denaturated for 10 min at 80 °C and incubated overnight at 37 °C. The next day, the sections were washed two times in 2× SSC.

Genome-wide amplification. Genome-wide amplification of DNA from microdissected crypts was performed as described previously[30]. The GenomePlex single cell whole-genome amplification kit (Sigma-Aldrich) was used according to the manufacturer's instructions with the following modifications: after tissue lysis and fragmentation of the genomic DNA, an amplification of the libraries was performed by adding 7.5 µl of 10× amplification master mix, 51 µl of nuclease-free water and 1.5 µl Titanium Taq DNA polymerase (Takara Bio Europe/Clontech) to 14 µl library mix. PCR conditions for amplification were denaturation at 95 °C for 3 min followed by 25 cycles, with each cycle consisting of a denaturation step at 94 °C for 30 s and an annealing and extension step at 65 °C for 5 min. DNA was purified using the GenElute PCR clean-up kit (Sigma-Aldrich). The quality of the amplification was evaluated using a multiplex PCR approach as previously described[31].

Array-comparative genomic hybridization. Array-CGH was carried out using a genome-wide oligonucleotide microarray platform (mouse genome CGH 44B microarray kit, Agilent Techologies). This array consists of approximately 43,000 60-mer oligonucleotide probes with a spatial resolution of about 22 kb. As reference DNA, we used amplified male DNA from the same mouse strain. Samples were labeled with the Bioprime array-CGH genomic labeling system (Invitrogen) according to the manufacturer's instructions. Briefly, 500 ng test DNA and reference DNA were differentially labeled with dCTP-Cy5 or dCTP-Cy3 (GE Healthcare). Slides were scanned using a microarray scanner, and images were analyzed using CGH Analytics 3.4.40 (both from Agilent Technologies) with the statistical algorithm ADM-2; the sensitivity threshold was 4.0. At least ten consecutive clones had to be aberrant to be scored by the software.

OLFM4 *in situ* hybridization. 8-µm-thick sections were rehydrated as described above. Afterward, the sections were treated with 0.2 M sodium chloride and proteinase K. Slides were postfixed, and sections were then demethylated with acetic anhydride and prehybridized. Hybridization was done in a humid chamber with 500 ng/ml freshly prepared digoxigenin (DIG)-labeled RNA probe of OLFM4. Sections were incubated for at least 48 h at 68 °C. The slides were washed, and incubation of the secondary anti-DIG antibody (Roche) was done at 4 °C overnight. The next day, sections were washed and developed using Nitro Blue Tetrazolium Chloride/5-Brom-4-Chlor-3-Indolyl-Phosphat.

28. Poon, S.S. *et al.* Telomere length measurements using digital fluorescence microscopy. *Cytometry* **36**, 267–278 (1999).
29. Chung, Y.J. *et al.* A whole-genome mouse BAC microarray with 1-Mb resolution for analysis of DNA copy number changes by array comparative genomic hybridization. *Genome Res.* **14**, 188–196 (2004).
30. Geigl, J.B. & Speicher, M.R. Single-cell isolation from cell suspensions and whole genome amplification from single cells to provide templates for CGH analysis. *Nat Protoc.* **2**, 3173–3184 (2007).
31. van Beers, E.H. *et al.* A multiplex PCR predictor for aCGH success of FFPE samples. *Br. J. Cancer* **94**, 333–337 (2006).